The Astronomical Journal, 155:215 (14pp), 2018 May https://doi.org/10.3847/1538-3881/aab9b8

Speckle Interferometry of Red Dwarf Stars

Brian D. Mason[1,6], William I. Hartkopf[1,6,8], Korie N. Miles[1,7], John P. Subasavage[2,3,6], Deepak Raghavan[4,6], and Todd J. Henry[5]
[1] U.S. Naval Observatory, 3450 Massachusetts Avenue, NW, Washington, DC 20392-5420, USA; brian.d.mason@navy.mil, william.hartkopf@navy.mil
[2] U.S. Naval Observatory, Flagstaff, AZ 86001, USA; jsubasavage@nofs.navy.mil
[3] 2310 E. El Segundo Boulevard, El Segundo, CA 90245, USA
[4] Center for High Angular Resolution Astronomy, Georgia State University, P.O. Box 3969, Atlanta, GA 30302-3969, Georgia; raghavan@astro.gsu.edu
[5] RECONS Institute, Chambersburg, PA 17201, USA; toddhenry28@gmail.com
Received 2017 November 20; revised 2018 March 19; accepted 2018 March 22; published 2018 April 27

Abstract

We report high-resolution optical speckle observations of 336 M dwarfs, which results in 113 measurements of the relative position of 80 systems and 256 other stars with no indications of duplicity. These are the first measurements for two of the systems. We also present the earliest measurements of relative position for 17 others. We include orbits for six of the systems, two revised and four reported for the first time. For one of the systems with a new orbit, G 161-7, we determine masses of 0.156 ± 0.011 and $0.1175 \pm 0.0079\ \mathcal{M}_{\odot}$ for the A and B components, respectively. All six of these new calculated orbits have short periods (between five and 38 years) and hold the promise of deriving accurate masses in the near future. For many other pairs we can establish their nature as physical or chance alignment, depending on their relative motion. Of the 80 systems, 32 have calculated orbits, 25 others are physical pairs, four are optical pairs, and 19 are currently unknown.

Key words: binaries: general – binaries: visual – stars: individual (G 161-7) – techniques: interferometric

1. Introduction

Double stars are those stars which, seen through the telescope, present themselves as two points of light. Some of these are physically associated with each other and are true bona fide *binary stars*, while others are chance alignments. While these "optical doubles" may prove troublesome as stray light complicates both photometry and astrometry, they are astrophysically inconsequential. The true binary nature of double stars can be detected through a variety of means, from wide systems found via common proper motion (CPM) to orbit pairs to the even closer systems, found through periodic variations in radial velocity or photometry. For generations, painstaking measurements of these stars have been collected in catalogs such as the Washington Double Star Catalog (WDS; Mason et al. 2001). The organization of significant data sets of multiple stars is critical to understanding the outcomes of the star formation process, as well as key to identifying which systems promise fundamental astrophysical parameters, e.g., masses.

Red dwarfs, specifically M dwarfs, are the most common stellar constituent of the Milky Way, accounting for three of every four stars (Henry et al. 2006). However, their binary fraction is quite low in comparison to other stars (~27%; Winters et al. 2015). The other end of the Main Sequence, the O stars, have a very high binary fraction (43/59/75% for runaway/field/cluster samples; Mason et al. 2009). Possible companions to an O star may include stars from the entire spectral sequence, while the only possible stellar companions to an M dwarf are lower-mass M dwarfs, brown dwarfs, or fainter evolved objects. Mass determinations of M dwarfs are poorly constrained;[9] observations of M dwarfs, for binary detection, orbit determination, and eventual mass determination, are of paramount importance. To improve the statistical basis for investigations of the nearest M dwarfs and to pinpoint systems worthy of detailed studies, in this paper we report high-resolution optical speckle observations of 336 M dwarfs. We report 113 resolved measurements of 80 systems, 19 of which have their first measure reported here, although all but two of those have their first published measure elsewhere.

2. Instrumentation and Calibration

Observing runs for this program are provided in Table 1, which includes the dates, telescopes and observers, a subset of the authors on this paper. The observing runs included many different projects, as speckle interferometry is a fast observing technique with up to 20 objects per hour observed and nightly totals of 120–220 stars, depending on hours of dark time. Most of the data that were not specific to this M dwarf program were massive stars (Mason et al. 2009) or exoplanet hosts (Mason et al. 2011). Other data are presented in Appendix A. The instrument used for these observations was the USNO speckle interferometer, which is described in detail in Mason et al. (2009, 2011). Briefly, the camera consists of two different microscope objectives giving different scales, interference filters of varying FWHM to allow fainter objects to be observed, Risley prisms that correct for atmospheric dispersion, and finally a Gen IIIc intensified charge coupled device (ICCD) capable of very short exposures necessary to take advantage of the "speckling" generated by atmospheric turbulence. Each observation represents the directed vector autocorrelation (Bagnuolo et al. 1992) of 2000+ individual exposures, each 1–15 ms long, depending on an object's brightness and the filter in use. As the speckles are an atmospheric effect

[6] Visiting Astronomer, Kitt Peak National Observatory and Cerro Tololo Inter-American Observatory, National Optical Astronomy Observatories, operated by Association of Universities for Research in Astronomy, Inc. under contract to the National Science Foundation.
[7] SEAP Intern.
[8] Retired.
[9] Although, thanks to work such as Benedict et al. (2016) it is getting better on the low-mass end.

Table 1
Observing Runs

Dates	Telescope	Observers
2005 Nov 8–13	KPNO 4 m	BDM and WIH
2006 Mar 9–13	CTIO 4 m	BDM and WIH
2007 Jul 30–Aug 10	KPNO 4 m	BDM, WIH and DR
2008 Jun 11–17	KPNO 4 m	BDM and DR
2010 Jan 23–25	CTIO 4 m	BDM and JPS
2010 Aug 1–3	CTIO 4 m	WIH and JPS

independent of the telescope, a larger telescope sees more turbulence cells and, therefore, more speckles. While a larger telescope can produce more correlations and a higher signal-to-noise ratio (S/N), it does not significantly change the magnitude limit. Brighter primary stars with $V < 11.5$ were observed with a *Strömgren y* filter (FWHM 25 nm centered on 550 nm). Stars fainter than this were observed with a *Johnson V* filter (FWHM 70 nm centered on 550 nm). The resolution limit with the 4 m telescope employed in these observations is 30 mas; however, when the wider filter was used, the resolution capability is degraded to 50 mas due to the greater atmospheric dispersion. The field of view is $1\farcs8$ centered on the target. The camera is capable of multiple observing modes, where wider pairs, if seen in the field, can be observed and measured using 2×2 or 4×4 binning.[10] However, this is only when the companion is seen or known a priori. In terms of the search for new companions, the field of-view is characterized as $1\farcs8 \times 1\farcs8$.

For calibration, a double-slit mask was placed over the "stove pipe" of the Kitt Peak National Observatory (KPNO) Mayall Reflector, and a known single star was observed. This application of the well-known experiment of Young allowed for the determination of scale without relying on binaries themselves to determine calibration parameters. The slit mask, at the start of the optical path, generates peaks based upon the slit-separation and the wavelength of observation. These peaks can be measured using the same methodology as a double star measure and, thus, generates a very precise scale for the charge coupled device (CCD). See McAlister et al. (1987) Section 4 and Figure 4 for further details. Multiple observations through the slit mask yield an error in the position angle zero point of $0\fdg20$ and a scale error of 0.357%. These "internal errors" are undoubtedly underestimates of the true errors of these observations. While this produces excellent calibration for the Mayall Reflector, due to small differences between it and the Cerro Tololo Inter-American Observatory (CTIO) Blanco Reflector, the double-slit-mask could not be placed on the CTIO 4 m "stove pipe." Because this option was not available on the CTIO Blanco Reflector, a large number of well-known equatorial binaries with very accurate orbits were observed with both telescopes to allow for the determination of more realistic global errors. Given the long time between some of these observations, wider pairs were observed with other telescopes that were slowly orbiting and well characterized, as well as linear pairs, were observed. This process prevented excessive extrapolation when measuring the scale of the observed field.

Speckle interferometry is a technique that is sensitive to changes in observing conditions, particularly coherence length (ρ_0) and time (τ_0). These typically manifest as a degradation of detection capability close to the telescope resolution limit or at larger magnitude differences between components. To ensure we reached our desired detection thresholds, a variety of systems with well-determined and characterized morphologies and magnitude differences were observed throughout each observing night. In all cases, results for these test systems indicated that our observing met or exceeded the desired separation and magnitude difference goals. Most, but not all, of the systems observed for characterizing errors or investigating detection space were presented in Mason et al. (2011). Others are presented in Appendix A below. Overall, our speckle observations are generally able to detect companions to M dwarfs from $30\,\mathrm{mas} < \rho < 1\farcs8$ if the $\Delta m_v < 2$ for M dwarfs brighter than $V = 11.5$. If fainter than this, the resolution of close pairs is degraded such that the effectively searched region is $50\,\mathrm{mas} < \rho < 1\farcs8$. Some observations and measurements were obtained during times of compromised observing conditions. Non-detections made at this time are not considered definitive and are not tabulated below.

[10] Increasing the field of-view to $3\farcs6$ or $7\farcs2$ in the horizontal or vertical and even larger by $\cos\theta$ along diagonals.

3. Results

Table 2 lists the astrometric measurements (T, θ, and ρ) of the observed red dwarf stars. The first two columns identify the system by providing the WDS designation (based on epoch-2000 coordinates) and discovery designation. Columns three through five give the epoch of observation (expressed as a fractional Julian year), the position angle (in degrees), and the separation (in seconds of arc). Colons indicate measures with reduced accuracy due to observing conditions. Note that the position angle has not been corrected for precession, and thus is based on the equinox for the epoch of observation. The sixth column indicates the number of observations contained in the mean position. Columns seven and eight list position angle and separation residuals (in degrees and arcseconds, respectively) to the orbit or rectilinear fit referenced in Column nine. Finally, the last column is reserved for notes for these systems.

While some of the published orbits may be premature and some linear determinations may reflect relative motion of an edge-on and/or long-period eccentric binary, these are nominally used to characterize each pair as physical and optical, respectively. Other pairs, as indicated in the notes to Table 2, are further classified as physical or optical based on the relative motion of the pair through inspection of their double star measures compared with the proper motion. The proper motion of these M dwarfs is typically large, therefore double star measures at approximately the same position over a time base of many years establishes the pair as physical through common proper motion. This assessment depends on the magnitude of the proper motion, the change in relative position, and the time between observations. This sort of analysis cannot be made for unconfirmed pairs.

For 21 of the pairs in Table 2 this represents the earliest measure. While the data presented in Table 2 has not been published before, their results had been shared with collaborators (Tokovinin et al. 2010, 2014, 2015, 2016, 2018; A. Tokovinin et al. 2019, in preparation; Hartkopf et al. 2012). In addition, the independent initiatives of others (Henry et al. 1999; Horch et al. 2010, 2011, 2012; Winters et al. 2011, 2017; Janson et al. 2012, 2014b, 2014a; Jodar et al. 2013; Riedel et al. 2014; Ward-Duong et al. 2015; Benedict et al. 2016) have further enhanced the capability to assess the physicality of these pairs and have enabled many of the orbits and linear solutions presented below.

Overall, 336 M dwarfs were observed. From these observations, we completed 113 measures of position angle and separation for 80 different pairs.

Table 2
Speckle Interferometric Measurements of Red Dwarf Pairs

WDS Designation	Discovery Designation			JY	θ	ρ	n	O−C	O−C	Reference	Notes
$\alpha\delta$ (2000)				2000.+	(°)	(″)		(°)	(″)		
(1)	(2)			(3)	(4)	(5)	(6)	(7)	(8)	(9)	(10)
00155−1608	HEI	299		7.6019	221.4:	0.374:	1	−1.4	0.008	Tokovinin et al. (2015)	
				10.5861	279.2	0.349	1	−1.1	−0.007	Tokovinin et al. (2015)	
00247−2653	LEI	1	AB	10.5889	33.1	1.356	1				
			AC	10.5889	23.3	1.464	1				
			BC	10.5889	307.7	0.264	1	−17.5	0.002	Köhler et al. (2012)	
00321+6715	VYS	2	AB	7.6021	173.2	3.945	1	−5.0	−0.031	Docobo et al. (2008)	
01245−3356	JAO	1	Aa,Ab	10.5891	42.8	2.019	1				(1)
01388−1758	LDS	838		5.8682	75.0	1.682	1	−0.6	−0.145	Kervalla et al. (2016)	
				7.5994	61.4	1.889	1	−0.4	−0.026	Kervalla et al. (2016)	
				10.5890	41.1	2.050	2	0.3	−0.029	Kervalla et al. (2016)	
02023−2634	LDS	65		10.5890	59.3	3.529	1				(1)
02288+3215	WOR	2		7.6021	101.9	0.266	1	−3.2	−0.015	Tamazian et al. (2005)	
03524−2253	HDS	484		10.5891	334.8	2.345	1				(3)
04073−2429	BEU	5		6.1963	79.7	0.776	1	−0.2	−0.004	Table 4	(2), (3), (4)
				10.0707	87.7	0.961	1	0.0	0.015	Table 4	
				10.5891	88.5	0.969	1	0.0	−0.002	Table 4	
05020+0959	HDS	654		6.1990	154.2	1.234	1				(5)
				10.0707	151.2	1.328	1				
05025−2115	DON	91	AB	10.0646	318.1	0.816	1	−0.5	0.008	Tokovinin et al. (2015)	
05069−2135	DON	93	BC	10.0707	141.0	0.774	1				(5)
05086−1810	WSI	72		6.1990	40.2	0.117	1				(2), (5)
05101−2341	WSI	121	Aa,Ab	10.0707	128.9	0.510	1	−0.0	−0.005	Table 4	(3), (6)
			BC	10.0707	307.6	1.819	1				(6)
05102−7236	WSI	122		10.0706	341.9	0.294	2				(6)
06293−0248	B	2601	AB	5.8691	43.7	1.243	1	−0.5	−0.121	Tokovinin et al. (2015)	
				10.0709	86.8	0.936	1	−0.1	−0.014	Tokovinin et al. (2015)	
06300−1924	WSI	123		10.0709	160.6	0.720	1	−0.4	−0.005	Table 4	(3), (6)
06308−7643	HEN	4		6.1964	38.1	1.187	1				(2)
				10.0710	54.0	1.243	1				
06445−4224	WSI	124		10.0710	267.3	1.744	1				
06523−0510	WSI	125	Ba,Bb	10.0682	149.6	0.175	1				(6)
06579+6220	HEN	2		5.8690	229.8	1.506	1				(2)
06579−4417	LPM	248		6.1964	87.2	1.238	1	−2.1	−0.107	Zirm 2003	
07048−3836	JAO	4		6.1964	268.4	2.406	1				(2)
				10.0697	268.7	2.371	2				
07120−3510	WSI	126		10.0697	33.3	1.016	2				(6)
07364+0705	HEN	3		5.8691	329.7	0.888	1				(5)
				6.1991	332.1	0.950	1				
				10.0708	355.4	0.806	1				
07549−2920	KUI	32		6.1994	77.4	1.010	1	−0.2	−0.001	Table 3	(7)
				10.0709	62.8	1.023	1	0.3	−0.002	Table 3	
08317+1924	DEL	1	Ba,Bb	6.1991	200.1	0.822	1				(2)
08589+0829	DEL	2		5.8691	230.4	0.208	1	2.0	−0.009	Tokovinin et al. (2015)	
				6.1991	2.7	0.101	2	5.5	−0.008	Tokovinin et al. (2015)	
				10.0708	81.6	0.576	1	0.3	−0.003	Tokovinin et al. (2015)	
09156−1036	MTG	2		10.0713	99.0	0.179	1	2.9	−0.002	Table 3	(7)
09313−1329	KUI	41		10.0713	318.6	0.653	1	0.2	0.001	Tokovinin et al. (2015)	
09370−2610	WSI	127		10.0713	283.8	0.391	1				(6)
10123−3124	WSI	128		10.0698	264.7	1.092	2				(6)
10430−0913	WSI	112		6.1967	266.8	0.477	1				(6)
				10.0685	unresolved		1				(8)
11105−3732	REP	21		10.0698	208.9	1.526	2	−0.7	0.007	Table 4	(3)
12290+0826	WSI	113		6.1968	190.2	0.275	1	−2.9	−0.020	Benedict et al. (2016)	
				10.0714	8.0	0.278	1	−2.1	−0.010	Benedict et al. (2016)	
12298−0527	B	2737		10.0686	60.3	8.106	1				(1)
12335+0901	REU	1		6.1968	219.4	0.167	1	−12.0	−0.002	Schulz et al. (1998)	
				8.4583	141.4	0.636	1	−2.3	0.003	Schulz et al. (1998)	
				10.0714	117.6	0.382	2	−5.5	−0.019	Schulz et al. (1998)	
12490+6607	DEL	4		8.4583	20.9	0.262	1				(2)
13317−0219	HDS	1895		10.5906	327.1	0.047	1	0.5	0.004	Hartkopf et al. (2012)	
13318+2917	BEU	17		8.4583	270.4	0.206	1				(2)
13320+3108	WOR	24		8.4611	125.5	0.134	1	8.1	−0.023	Docobo et al. (2000)	
13422−1600	WSI	114		8.4583	82.5	0.513	1	−0.3	−0.001	Table 4	(2), (3), (4), (6)

Table 2
(Continued)

WDS Designation	Discovery Designation			JY	θ	ρ	n	O−C	O−C	Reference	Notes
$\alpha\delta$ (2000)				2000.+	(°)	(″)		(°)	(″)		
(1)	(2)			(3)	(4)	(5)	(6)	(7)	(8)	(9)	(10)
				10.0700	71.5	0.504	2	0.0	0.002	Table 4	
				10.5906	67.6	0.501	1	−0.1	−0.003	Table 4	
14121−0035	WSI	129	Aa,Ab	10.5906	171.8	0.615	1				(2), (6)
14170+3143	DEL	5		8.4583	240.4	0.644	1				
14540+2335	REU	2		8.4583	101.8	1.130	1	−6.9	0.032	Heintz (1990)	(7)
								−0.8	0.015	Table 3	
				10.5906	98.7	1.076	2	−7.2	−0.033	Heintz (1990)	
								−0.4	−0.012	Table 3	
14575−2125	HN	28	Ba,Bb	6.1943	218.3	0.156	1	7.2	−0.038	Forveille et al. (1999)	
16093−2222	WSI	130		10.5881	189.7	1.116	2				(6)
16268−1724	WSI	131		10.5881	181.1	0.506	1				(2), (6)
16302−1440	WSI	132		10.5881	211.0	0.412	1				(2)
16305−3634	WSI	133		10.5880	246.9	2.015	1				(2)
16453−3848	RST	1900	Aa,Ab	10.5854	232.0	0.503	2				(5)
16555−0820	KUI	75	AB	6.2000	220.2	0.229	1	−1.0	−0.002	Söderhjelm (1999)	⋆
				8.4559	115.5	0.219	1	−1.2	−0.003	Söderhjelm (1999)	
16584+1358	YSC	61		6.1971	300.5	0.859	1				(2), (6)
				8.4585	293.6	0.825	1				
				10.5881	286.0	0.765	1				
17077+0722	YSC	62		6.1971	243.1	0.146	1	−0.8	−0.003	Table 3	(6), (7)
17119−0151	LPM	629		10.5883	219.9	0.808	1	−17.6	−0.072	Söderhjelm (1999)	(7)
								−0.5	−0.015	Table 3	
17121+4540	KUI	79	AB	7.6013	260.7	0.980	1	−1.3	−0.006	Hartkopf et al. (1996)	
				8.4613	254.5	1.049	4	−0.0	−0.015	Hartkopf et al. (1996)	
17372+2754	KUI	83	AB	7.6041	349.5	0.238	1	−0.3	0.002	Mason & Hartkopf (2012)	
				8.4527	332.1	0.231	5	0.2	0.001	Mason & Hartkopf (2012)	
17465+2743	AC	7	BC	7.6014	232.6	1.109	1	0.6	0.008	Prieur et al. (2014)	
				8.4523	238.2	1.134	3	2.0	0.002	Prieur et al. (2014)	
18210−0101	VKI	46		6.1974	11.7	1.471	1				
				7.5879	9.9	1.452	2				
				8.4587	10.6	1.451	1				
				10.5883	8.9	1.454	1				
18566−4705	WSI	134		10.5884	137.9	1.224	1				(2)
19074+3230	KUI	90	Ca,Cb	7.6014	292.0	0.107	1	29.1	−0.247	Ségransan et al. (2000)	
				8.4587	78.8	0.190	1	−12.7	−0.093	Ségransan et al. (2000)	
19121+0254	AST	1		6.1974	207.7	0.134	1	4.4	−0.004	Benedict et al. (2016)	
				7.6014	116.9	0.125	1	1.7	0.004	Benedict et al. (2016)	
19131−3902	WSI	135		10.5884	152.4	0.889	2				(2), (6)
19449−2338	MTG	4		10.5911	347.9	0.790	1	−0.1	−0.002	Table 3	(7)
20100−2802	BRG	30		10.5911	281.3	0.632	1				
20428−5737	WSI	136		10.5885	338.3	2.240	1				(2)
20452−3120	LDS	720	BC	10.5886	157.7	2.437	1	−1.4	0.026	Hartkopf & Mason (2014)	
21109+2925	BAG	29		7.6018	25.3	0.124	1	−4.6	−0.008	Balega et al. (2010)	
21313−0947	BLA	9		7.5992	147.6	0.198	1	−2.9	−0.002	Benedict et al. (2016)	
21492−4133	WTR	1		10.5913	139.4	2.762	1	−0.4	0.024	Table 4	(3)
22173−0847	BEU	22	Ba,Bb	10.5886	319.8	0.923	1				
22280+5742	KR	60	AB	7.5919	48.3	2.206	3	−1.6	0.010	Heintz (1986)	
				8.4590	42.1	2.081	1	−0.1	0.005	Heintz (1986)	
22284−2553	WSI	137	Aa,Ab	10.5887	243.6	0.229	2				(6)
	LDS	2944	AB	10.5887	215.4	3.336	1				
22385−1519	BLA	10		7.5992	151.0	0.193	1	43.1	0.058	Ségransan et al. (2000)	
				8.4590	354.7	0.411	1	5.4	−0.063	Ségransan et al. (2000)	
23036−4651	WSI	139		10.5887	331.7	0.275	1				(6)
23455−1610	MTG	5		10.5916	192.9	0.508	1				
23597−4405	WSI	140		10.5887	119.6	0.263	1				(6)

Note. ⋆: System used in characterizing errors or investigating detection space. (1) Based on the very similar proper motions of the components and the lack of significant change in the relative position, this pair is deemed physical. (2) Based on the high proper motion of the primary and the lack of significant change in the relative position, this pair is deemed physical. (3) New linear solution. Unless indicated otherwise, counted as optical. See Table 4. (4) Preliminary elements were published in Miles & Mason (2016). (5) Measures indicate non-linearity, i.e., physical. However, current data insufficient for orbit determination. Continued observation justified. (6) First observation of this pair. (7) New orbit. See Table 3. (8) Pair unresolved on date of observation. The secondary could have moved to closer than $0\farcs03$ or the $\Delta m > 2.0$ due to variability of one or both components, or this may indicate the companion was optical due and no longer visible due to the high proper motion of the primary.

4. Analysis of Resolved Doubles

4.1. New Orbital Solutions

All of the orbits were computed using the "grid search" routine described in Hartkopf et al. (1989); weights are applied based on the methods described by Hartkopf et al. (2001a). Briefly, weights of the individual observations are evaluated based on the separation relative to the resolution capability of the telescope (larger telescopes produce more accurate data), the method of observation (e.g., micrometry, photography, interferometry, etc.), whether the published measure is a mean of multiple nights, and if the measurer made any notes regarding the quality of the observation. Elements for these systems are given in Table 3, where columns (1), (2), and (3) give the WDS and discovery designations, followed by an alternate designation; columns (4)–(10) list the seven Campbell elements: P (period, in years), a (semimajor axis, in arcseconds), i (inclination, in degrees), Ω (longitude of node, equinox 2000.0, in degrees), T_0 (epoch of periastron passage, in fractional Julian year), e (eccentricity), and ω (longitude of periastron, in degrees). Formal errors are listed with each element. Columns (11) and (12) provide the orbit grade (see Hartkopf et al. 2001a) and the reference for a previous orbit determination, if one exists. Orbit grades are on a 1–5 scale. In the case of the orbits presented here, a grade of 3 indicates the orbit is "reliable," 4 is "preliminary" and "5" is "indeterminate." In all of the cases here, the numbers are indicative of the small number of observations and incomplete phase coverage.

Figure 1 illustrates the new orbital solutions for the six systems with orbits that are presented here, plotted together with all of the published data in the WDS database as well as the previously unpublished data from Table 2. In each of these plots, micrometric observations are indicated by plus signs, and photographic measures by asterisks; *Hipparcos* measures are indicated by the letter "H," conventional CCD measures by triangles, interferometric measures by filled circles, and the new measures presented in Table 2 are indicated with stars. "O–C" lines connect each measure to its predicted position along the new orbit (shown as a thick solid line). Dashed "O–C" lines indicate measures given zero weight in the final solution. A dotted–dashed line indicates the line of nodes, and a curved arrow in the lower-right corner of each figure indicates the direction of orbital motion. The scale, in arcseconds, is indicated on the left and bottom of each plot. Finally, if there is a previously published orbit it is shown as a dashed ellipse. The sources of those orbits are listed in the final column of Table 3.

The orbital periods of all six pairs (three of which have very high eccentricities; >0.7) are all quite short, from 5 to 38 year, and have small semimajor axes (0.″2–0.″9). The potential for improvement of the orbits and precise mass determinations for these pairs, all with large parallaxes, is excellent, especially for precise high angular resolution work with large aperture instruments. The errors of some of the earlier micrometry measures are quite high (e.g., WDS14540+2335), and are given quite low weight in the orbit. However, these historic observations can be quite helpful, especially in determining the orbital period. The most interesting of these six pairs is discussed in detail below, while the remaining five are noted in Section 6.

4.1.1. G 161-7

The M dwarf star G 161-7 (alternatively known as LHS 6167 or NLTT 21329) was first resolved as a double with adaptive optics by Montagnier et al. (2006), who resolved the pair on two occasions. If the resolved optical companion of G 161-7 were simply a chance alignment with small proper motion, then the high proper motion of G 161-7 would result in a relative shift of 1.″6 between the two components. However, the companion continues to stay quite close, making this a very likely physical pair. While maintaining their proximity, large changes in the position angle of the companion demonstrated that the orbital period was short. Observed by this effort in 2010 (Table 2) the measures were also supplemented by Janson et al. (2014b), who observed it with "lucky imaging" and were able to split the pair as well as determine a mass ratio: 0.57 ± 0.05. Lately, it has been regularly observed by the SOAR-Speckle program (Tokovinin et al. 2015, 2016, 2018; A. Tokovinin et al. 2019, in preparation).

Bartlett et al. (2017) measured the parallax (103.33 ± 1.00 mas) to this nearby pair and also made an estimate of ~4 year for the orbital period. Taking the available relative astrometry, an orbital solution with a period just over 5 year quickly converged (see Table 3 and Figure 1). With the parallax a mass sum of $0.273 \pm 0.018\ \mathcal{M}_\odot$ is determined, and with the mass ratio individual masses of 0.156 ± 0.011 and $0.1175 \pm 0.0079\ \mathcal{M}_\odot$ are determined for A and B, respectively. While *Gaia* parallax should be quite precise for this pair, the errors of the orbit, already under 2%, can be improved with the accumulation of more data filling in unobserved regions of the orbit. With this, the orbital elements and, hence, the mass errors will improve. This pair is the best example of what we hope this effort will ultimately achieve.

4.2. New Linear Solutions

Inspection of all observed pairs with either a 30° change in their relative position angles or a 30% change in separations since the first observation cataloged in the WDS revealed six pairs with motion that seemed linear. These apparent linear relative motions suggest that these pairs are either composed of physically unrelated stars or have very long orbital periods. Linear elements to these doubles are given in Table 4, where Columns one and two give the WDS and discoverer designations and Columns three to nine list the seven linear elements: x_0 (zero point in x, in arcseconds), a_x (slope in x, in $''$/yr), y_0 (zero point in y, in arcseconds), a_y (slope in y, in $''$/yr), T_0 (time of closest apparent separation, in years), ρ_0 (closest apparent separation, in arcseconds), and θ_0 (position angle at T_0, in degrees). See Hartkopf & Mason (2015) for a description of all terms.

Figure 2 illustrates these new linear solutions, plotted together with all of the published data in the WDS database, as well as the previously unpublished data from Table 2. Symbols are the same as in Figure 1. In the case of linear plots, the dashed line indicates the time of closest apparent separation. As in Figure 1, the direction of motion is indicated at the lower right of each figure. As the plots and solutions are all relative, the proper motion (μ) difference is assumed to be zero.

Table 5 gives ephemerides for each orbit or linear solution over the years 2018 through 2023, in annual increments.

Table 3
New Orbital Elements

WDS (Figure No.) (1)	Discoverer Designation (2)		Other Designation (3)	P (years) (4)	a ($''$) (5)	i (°) (6)	Ω (°) (7)	T_o (years) (8)	e (9)	ω (°) (10)	Grade (11)	Previous Orbit (12)
07549−2920	KUI	32	LHS 1955	32.3 ± 1.5	0.870 ± 0.029	131.7 ± 2.6	125.1 ± 7.5	1996.2 ± 1.1	0.686 ± 0.020	257.6 ± 2.1	4	first orbit
09156−1036	MTG	2	LHS 6167	5.075 ± 0.016	0.1981 ± 0.0021	117.00 ± 0.66	117.0 ± 1.2	2014.032 ± 0.036	0.4541 ± 0.0098	270.94 ± 0.75	3	first orbit
14540+2335	REU	2	GJ 568	31.45 ± 0.42	0.626 ± 0.033	143. ± 15.	303. ± 22.	1992.61 ± 0.53	0.839 ± 0.046	25. ± 25.	4	Heintz (1990)
17077+0722	YSC	62	GJ 1210	14.026 ± 0.081	0.2969 ± 0.0025	114.95 ± 0.79	241.04 ± 0.48	2006.486 ± 0.048	0.5128 ± 0.0096	19.5 ± 1.6	3	first orbit
17119−0151	LPM	629	GJ 660	34.582 ± 0.053	0.7663 ± 0.0062	20.0 ± 2.1	154.5 ± 7.7	1988.39 ± 0.12	0.1830 ± 0.0080	210.3 ± 7.5	3	Söderhjelm (1999)
19449−2338	MTG	4	LP 869-26	33.0 ± 2.6	0.459 ± 0.015	123.2 ± 9.0	171.7 ± 8.7	2023.21 ± 0.55	0.804 ± 0.056	359. ± 19.	5	first orbit

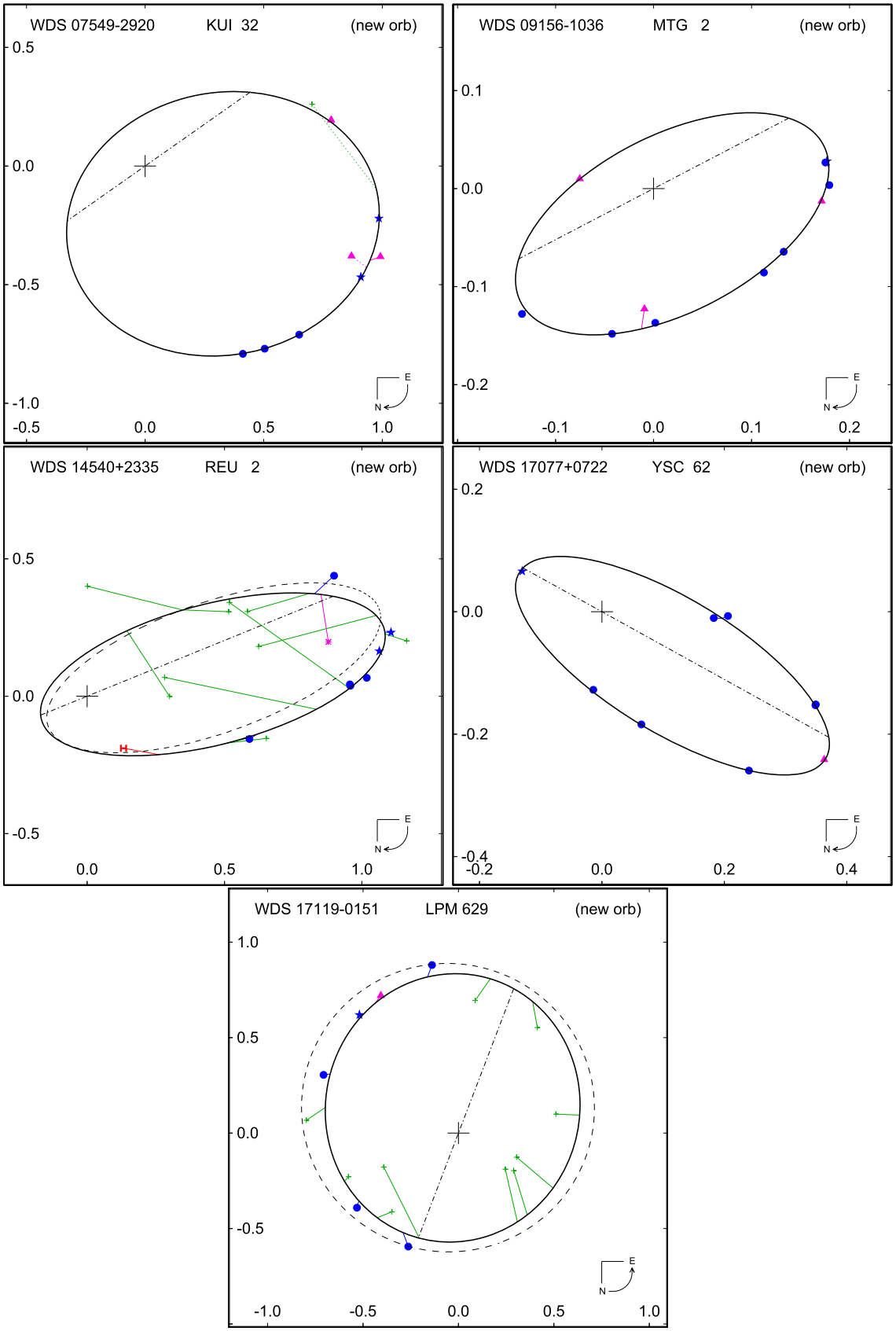

Figure 1. New orbits for the systems listed in Table 3 and all data in the WDS database and Table 2. Micrometric observations are indicated by plus signs, and photographic measures by asterisks; *Hipparcos* measures are indicated by the letter "H," conventional CCD measures by triangles, interferometric measures by filled circles, and the new measures presented in Table 2 are indicated with stars. "O–C" lines connect each measure to its predicted position along the new orbit (shown as a thick solid line). Dashed "O–C" lines indicate measures given zero weight in the final solution. A dotted–dashed line indicates the line of nodes, and a curved arrow in the lower-right corner of each figure indicates the direction of orbital motion. The scale, in arcseconds, is indicated on the left and bottom of each plot. Finally, if there is a previously published orbit, it is shown as a dashed ellipse.

Table 4
New Linear Elements

WDS	Discoverer Designation			x_0	a_x	y_0	a_y	T_0	ρ_0	θ_0
α, δ (2000)				($''$)	($''$/yr)	($''$)	($''$/yr)	(yr)	($''$)	(deg)
(1)	(2)			(3)	(4)	(5)	(6)	(7)	(8)	(9)
04073−2429	BEU	5		0.250114	0.044070	−0.435759	0.025295	1994.338	0.502	29.85
05101−2341	WSI	121	Aa,Ab	0.095884	−0.022807	0.397173	0.005506	2023.416	0.409	166.43
06300−1924	WSI	123		−0.053621	−0.028649	0.678105	−0.002265	2020.057	0.680	184.52
11105−3732	REP	21		−1.120781	0.010277	0.798936	0.014417	1973.890	1.376	234.52
13422−1600	WSI	114		0.467162	−0.023533	−0.195311	−0.056288	2010.631	0.506	67.31
21492−4133	WTR	1		1.935622	0.042888	1.922322	−0.044115	2012.841	2.665	136.81

Table 5
Ephemerides

WDS	Discoverer			2018.0		2019.0		2020.0		2021.0		2022.0		2023.0	
Designation	Designation			$\theta°$	ρ''	$\theta°$	ρ''	$\theta°$	ρ''	$\theta°$	ρ''	$\theta°$	ρ''	$\theta°$	ρ''
04073−2429	BEU	5		97.2	1.321	98.0	1.370	98.8	1.419	99.5	1.469	100.2	1.519	100.8	1.569
05101−2341	WSI	121	Aa,Ab	149.2	0.428	152.2	0.422	155.3	0.416	158.5	0.412	161.8	0.410	165.1	0.409
06300−1924	WSI	123		179.8	0.693	182.2	0.694	184.7	0.697	187.1	0.700	189.5	0.705	191.8	0.712
07549−2920	KUI	32		28.1	0.894	22.9	0.867	17.2	0.838	11.2	0.805	4.6	0.770	357.3	0.729
09156−1036	MTG	2		316.4	0.184	247.9	0.062	103.8	0.180	64.1	0.148	2.6	0.139	318.9	0.183
11105−3732	REP	21		204.9	1.583	204.4	1.591	203.8	1.600	203.3	1.609	202.8	1.619	202.2	1.628
13422−1600	WSI	114		26.6	0.710	23.2	0.756	20.2	0.804	17.5	0.854	15.2	0.906	13.1	0.959
14540+2335	REU	2		82.6	0.753	78.8	0.673	73.8	0.581	66.7	0.476	55.2	0.356	30.2	0.219
17077+0722	YSC	62		2.6	0.147	303.7	0.109	252.1	0.148	202.6	0.095	102.1	0.134	78.6	0.256
17119−0151	LPM	629		295.9	0.681	308.4	0.666	321.4	0.653	334.9	0.639	349.0	0.627	3.6	0.616
19449−2338	MTG	4		335.0	0.490	331.3	0.416	325.9	0.331	316.3	0.233	290.2	0.124	193.1	0.085
21492−4133	WTR	1		130.4	2.736	129.1	2.742	127.8	2.748	126.6	2.756	125.3	2.766	124.1	2.776

Columns (1) and (2) are the same identifiers as in the previous tables, while columns (3+4), (5+6), ... (13+14) give predicted values of θ and ρ, respectively, for the years 2018.0, 2019.0, etc., through 2023.0. All of the orbit pairs are relatively fast moving, with mean motions of more than $6°$/yr. Notes to individual systems are given in Section 6.

5. M Dwarfs with No Companion Detected

The selection of systems for this project was not blind and preference was given to systems previously known as double or having parallax data from the CTIOPI program (Jao et al. 2005) that seemed to indicate duplicity. Therefore, any duplicity rate that we determine would be enriched and not representative of stars of this type. Despite this preselection, there were a large number of targets observed for which we did not detect a companion.

Table 6 provides the complete list of unresolved red dwarfs obtained on these observing runs. In some cases, known companions are not detectable due to the separation being wider than the field of view of $1\farcs8$, or the magnitude difference being larger than detectable by the optical speckle camera. Due to the faintness of the primary targets, the companion must have $\Delta m < 2$ mag and 30 mas $< \rho < 1\farcs8$. In this case, the upper limit is set by the minimum field of view when the object is centered for detection of unknown companions. As seen in Table 2, wider systems can be measured with a priori knowledge of the system or if they are seen while pointing the telescope. The usual procedure after moving the telescope to the approximate field was to step through larger fields of view obtained through 4×4 or 2×2 binning en route to a final un-binned field of about 6 mas/pixel. Data could be taken in these binned fields to obtain measures of wider pairs. In some cases, pairs were too widely separated to be measured; often, for these both components were observed separately. Finally, as some of these targets are rather faint, an interference filter with a significantly larger FWHM (*Johnson V* as opposed to *Strömgren y*) was used to allow enough photons to permit detection. However, use of this filter compromises the detection of the closest pairs. For these we set a lower separation limit of 50 mas. The cases where this filter was used are noted in Table 6.

All individual observations, including a complete listing of each measure identifying the date of observation, resolution limit, filter, and telescope, are given in the Catalog of Interferometric Measurements of Binary Stars.[11] Notes to individual systems reported here are provided in Section 6.

6. Notes to Individual Systems

WDS04073−2429 = BEU 5 = LHS 1630 (resolved, linear, in WDS): The proper motion (UCAC5; Zacharias et al. 2017) is 673.1 mas yr^{-1}, which seems to indicate the components are moving together with small changes in relative position, so the pair is classified as physical. However, their relative motion can be fit by a line (see Section 4.2, Table 4 and Figure 2). More data obtained over several years may determine if we have a companion that is optical, or if we happen to be catching the orbit on a long near-linear segment.

WDS05000−0333 = JNN 29 = SCR J0459−0333 (unresolved, in WDS): The companion has been measured multiple

[11] See Hartkopf et al. (2001b). The online version (http://ad.usno.navy.mil/wds/int4.html) is updated frequently.

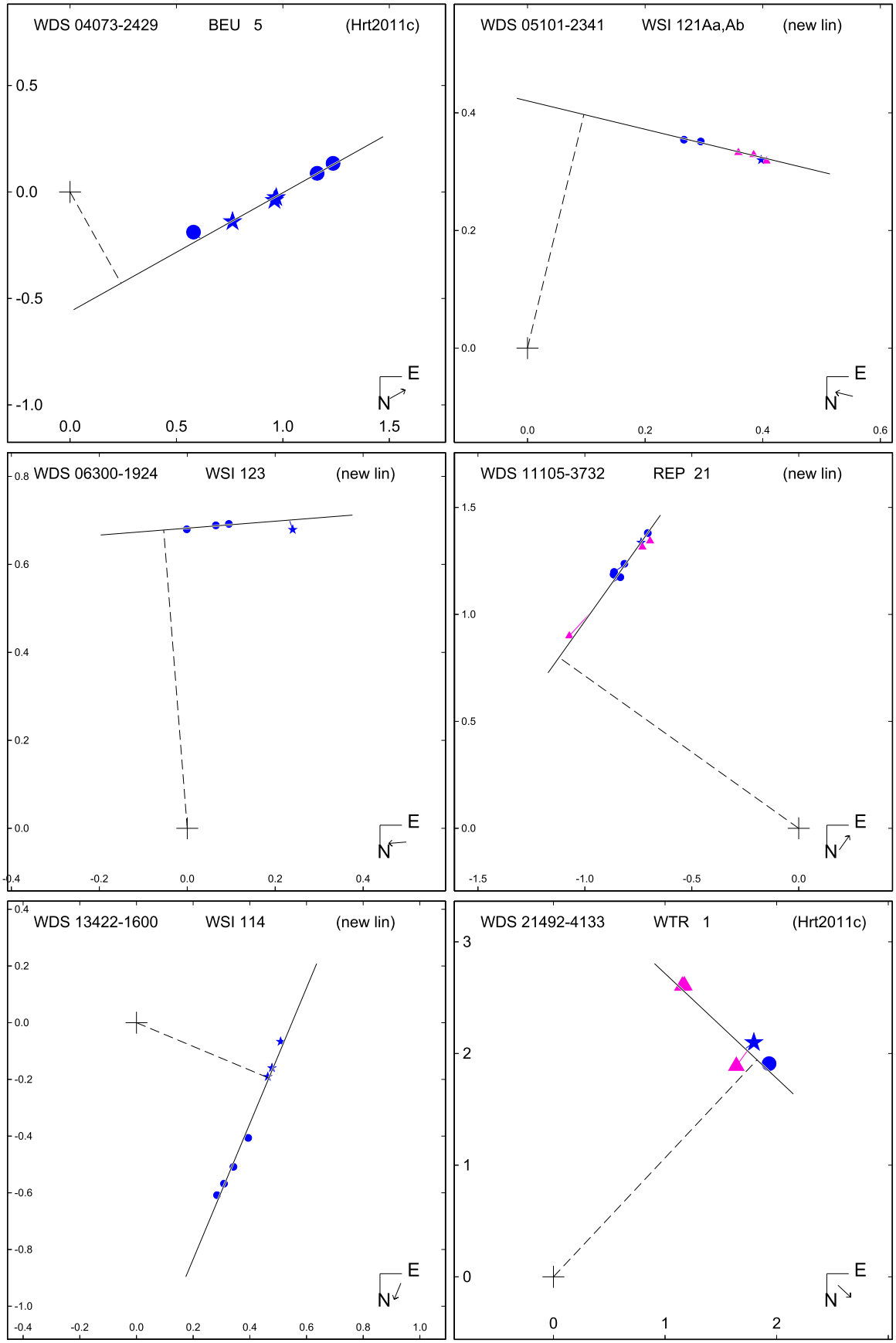

Figure 2. New linear fits for the systems listed in Table 4 and all of the data in the WDS database and Table 2. Symbols are the same as Figure 1. "O–C" lines connect each measure to its predicted position along the linear solution (shown as a thick solid line). An arrow in the lower-right corner of each figure indicates the direction of motion. The scale, in arcseconds, is indicated on the left and bottom of each plot.

times, but only through red filters (Janson et al. 2012, 2014a). It may be too faint in *Johnson V*.

WDS05174−3522 = TSN 1 = L 449-001 (unresolved, in WDS): The companion has only been measured with *HST*-Fine Guidance Sensors (FGS) once at 47 mas (Riedel et al. 2014), closer than our limit here with the *Johnson V* filter. This known pair is worth additional observations with large aperture high angular resolution techniques.

WDS06523−0510 = GJ 250 (resolved, in WDS): The wide CPM pair WNO 17AB has many measures. Two unconfirmed companions to B have been measured: WSI 125Ba,Bb, measured only in Table 2, and the much wider IR companion TNN 6BC, measured in Tanner et al. (2010). It is unknown if either of these are physical. We crudely estimate the Δm in *V* as 0.5 for the Ba,Bb pair.

WDS07549−2920 = KUI 32 = LHS 1955 (resolved, orbit, in WDS): The first orbit of this pair. Based on these elements and the parallax (74.36 ± 1.13 mas; Winters et al. 2015), the resulting mass sum of $1.54 \pm 0.37\ \mathcal{M}_{\odot}$ is suspiciously large. (see Section 4.1, Table 3 and Figure 1). It is possible that these preliminary orbital elements may aid future determinations and the planning of observing.

WDS08272−4459 = JOD 5 = LHS 2010 (unresolved, in WDS): The companion has only been measured once in the red (914 mas in 2008; Jodar et al. 2013). The companion is either too faint in the *Johnson V* observation or the companion is optical and has moved to a separation too wide for detection.

WDS08317+1924 = BEU 12Aa,Ab = GJ 2069 (unresolved, in WDS): This pair of the multiple system has only been measured in the red or infrared. The companion is likely too faint in this *Johnson V* measurement for detection. The Ba,Bb pair is resolved in Table 3. AB is CPM but is too wide for measurement here.

WDS10121−0241 = DEL 3 = GJ 381 (unresolved, in WDS): The companion has only been measured in the red or infrared. It is likely too faint in this *Johnson V* measurement for detection.

WDS10430−0913 = WSI 112 = WT 1827 (resolved, in WDS): The companion is measured only in Table 2. It is unknown if it is physical. We crudely estimate the Δm in *V* as 1.7.

WDS11105−3732 = REP 21 = TWA 3 (resolved, orbit or linear, in WDS): The proper motion (UCAC4; Zacharias et al. 2013) is 107.3 mas yr^{-1}. While orbits with periods ranging from 236 to 800 year have been determined, "the χ^2 from the orbit fit was indistinguishable from the linear fit" (Kellogg et al. 2017). The solution presented in Section 4.2, Table 4, and Figure 2 is a linear fit to the data. Only time will tell if we have a companion that is optical or if we happen to be catching the orbit on a long near-linear segment.

11354−3232 = GJ 433 (unresolved, not in WDS): Detected as a 500-day pair by *Hipparcos* (ESA 1997). However, according to Delfosse et al. (2013), radial velocity coverage eliminates the *Hipparcos* result and the system just has one short-period planet.

WDS13422−1600 = WSI 114 = LHS 2783 (resolved, linear, in WDS): Given the high proper motion of the PPMXL (508.6 mas yr^{-1}; Roeser et al. 2010) and that from the CTIOPI (503.6 mas yr^{-1}; Bartlett et al. 2017), it would indicate that the stars are moving together. The measures can be fit by a line (see Section 4.2, Table 4 and Figure 2), and thus far do not seem to support the estimated period of 52 year from Bartlett et al. (2017). However, based on this orbital period, the parallax, and an assumed total mass of 0.5 $\mathcal{M}_{\odot}$, a″ would be 0.″28, not too different from our measurements (Table 2) of about 0.″5. This tends to support the supposition that we are looking at a physical pair observed when the relative motion only appears to be linear. The pair should be monitored for variation from linearity.

WDS14540+2335 = REU 2 = GJ 568 (resolved, orbit, in WDS): The orbit of Heintz (1990) is improved here. Based on these elements and the parallax (98.40 ± 4.42 mas; van Leeuwen 2007), the resulting mass sum is $0.261 \pm 0.083\ \mathcal{M}_{\odot}$. See Section 4.1, Table 3 and Figure 1.

15301−0752 = G 152-31 (unresolved, not in WDS): This 5.96 year pair of Harrington & Dahn (1988) should be resolvable ($a'' = 496$ mas assuming $\Sigma\ \mathcal{M} = 0.5\ \mathcal{M}_{\odot}$); therefore, it is assumed the Δm is higher than 2.5 and observation with a technique with a greater Δm sensitivity, such as adaptive optics, is appropriate.

WDS16240+4822 = HEN 1Aa,Ab = GJ 623 (unresolved, in WDS): The companion has only been measured in the infrared or with *HST*-FGS. It likely has too large a Δm for *V* band detection here.

WDS17077+0722 = YSC 62 = GJ 1210 (resolved, orbit, in WDS): This is the first orbit for this pair, the first published measure (Horch et al. 2010) of which was made two years after that presented in Table 2. Based on these elements and the parallax (78.0 ± 5.3 mas; van Altena et al. 1995), the resulting mass sum is $0.280 \pm 0.067\ \mathcal{M}_{\odot}$. See Section 4.1, Table 3 and Figure 1.

WDS17119−0151 = LPM 629 = GJ 660 (resolved, orbit, in WDS): The orbit of Söderhjelm (1999) is improved here. Based on these elements and the parallax (98.19 ± 12.09 mas; van Leeuwen 2007), the resulting mass sum is $0.40 \pm 0.16\ \mathcal{M}_{\odot}$. See Section 4.1, Table 3 and Figure 1.

WDS18387−1429 = HDS 2641 = GJ 2138 (unresolved, in WDS): The companion was measured by *Hipparcos* (ESA 1997) at 107 mas and $\Delta H_p = 0.41$. It would be expected to be resolved in our observation if near this location. Because it is not, the pair has either closed under 50 mas, was optical, or was a false detection.

WDS19449−2338 = MTG 4 = LP 869-26 (resolved, orbit, in WDS): This is the first orbit for this pair. Based on these elements and the parallax (67.87 ± 1.1 mas; Bartlett et al. 2017), the resulting mass sum is $0.283 \pm 0.086\ \mathcal{M}_{\odot}$. See Section 4.1, Table 3 and Figure 1.

23018−0351 = GJ 886 (unresolved, not in WDS): The 468.1 day pair of Jancart et al. (2005) may have a separation close to our resolution limit, or slightly under it ($a'' = 50$ mas assuming $\Sigma\ \mathcal{M} = 0.5\ \mathcal{M}_{\odot}$). The Δm is unknown and may also be too high for our detection. This pair is worthy of additional observation.

7. Conclusions

In this paper, we report high-resolution optical speckle observations of 336 M dwarfs that resulted in 113 resolved measurements of 80 systems and 256 other stars that gave no indication of duplicity within the detection limits of the telescope/system. We calculate orbits for six systems, two of which were revised and four which are first-time orbits. All have short periods, 5–38 year, and these data may eventually assist in determining accurate masses.

Table 6
Null Companion Detection ($\rho < 0\farcs03$) for Red Dwarf Stars

Unresolved at KPNO (2005.8625−2005.8692)					
G 221-022 (1)	GJ 53 (6)	GJ 84 (3)	GJ 105 (2)	GJ 164 (6)	GJ 222 (2)
GJ 319 (2)	GJ 381 (1), (3)	GJ 395 (4)	GJ 860 (4)	GJ 886 (5)	HIP 2552 (3)
Unresolved at CTIO (2006.1882−2006.2001)					
AP COL (4)	G 88-019 (1)	G 99-049 (1)	G 152-031 (1), (5)	GJ 300 (1), (4)	GJ 319 (2)
GJ 381 (1), (3)	GJ 433 (5)	GJ 494 (6)	GJ 680 (4)	GJ 1068 (1)	GJ 1093 (1)
GJ 1103 (1), (4)	GJ 1123 (1)	GJ 1128 (1)	GJ 1203 (1)	GJ 1207 (1)	GJ 1215 (1)
GJ 2069 (1)	GJ 2130 (1), (4)	LHS 288 (1)	LHS 337 (1)	LHS 382 (1)	LHS 1723 (1)
LHS 2460 (1)	SCR 1138−7721 (1)	WT 0460 (1), (6)			
Unresolved at KPNO (2007.5876−2007.6076)					
HIP 2552 (6)	GJ 53 (6)	GJ 105 (2)	GJ 623 (3)	GJ 1245 (1), (2)	LHS 501 (1), (4)
LHS 1050 (1)					
Unresolved at KPNO (2008.4473−2008.4618)					
G 169-029 (1)	G 182-041 (1)	GJ 465 (1)	GJ 555 (1)	GJ 581 (1)	GJ 595 (1)
GJ 623 (3)	GJ 628 (2)	GJ 643 (1), (4)	GJ 688 (2)	GJ 802 (2)	GJ 849
GJ 876	GJ 1224 (1)	L 1209-006 (1), (2)	HIP 103039 (1)	L 755-019 (1)	LHS 2520 (1)
LHS 2836 (1)	LHS 2880 (1)	LHS 3056 (1)	LHS 3076 (1), (4)	LHS 3799 (1)	LTT 15483 (1)
SCR 2009−0113 (1)					
Unresolved at CTIO (2010.0654−2010.0712)					
CD−268623A (1)	CD−268623B (1)	G 161-071 (1)	GJ 231.1 (1), (2)	GJ 357 (1)	GJ 358 (1)
GJ 367 (1)	GJ 406 (1)	GJ 433 (5)	GJ 442B (1)	GJ 479 (1)	GJ 480.1 (1)
GJ 1061 (1)	GJ 1065 (1)	GJ 1157 (1)	HD 268899 (1)	L 032-009A	L 032-009B
L 449-001 (1), (3)	L 749-034 (1)	LEHPM 13427 (1)	LDS 3975A (1)	LDS 3975B (1)	LHS 205 (1)
LHS 292 (1)	LHS 1561 (1)	LHS 1731 (1)	LHS 2010 (3)	LHS 2071 (1)	LHS 2122 (1)
LHS 2567 (1), (4)	LTT 2816 (1)	NLTT 25158 (1)	NLTT 30359 (1)	PM J 11413−3624 (1)	SCR 0336−2619 (1)
SCR 0424−0647 (1)	SCR 0432−5741 (1)	SCR 0459−0333 (1), (3)	SCR 0500−7157 (1)	SCR 0506−4712 (1)	SCR 0509−4209 (1)
SCR 0509−4325 (1)	SCR 0513−7653 (1)	SCR 0522−0606 (1)	SCR 0526−4851 (1)	SCR 0527−7231 (1)	SCR 0529−3239 (1)
SCR 0533−4257 (1)	SCR 0631−8811 (1)	SCR 0635−6722 (1)	SCR 0643−7003 (1)	SCR 0702−6102 (1)	SCR 0708−4709 (1)
SCR 0713−0511 (1)	SCR 0717−0500 (1)	SCR 0736−3024 (1)	SCR 0740−4257 (1)	SCR 0754−3809 (1)	SCR 0757−7113 (1)
SCR 0805−5912 (1)	SCR 0833−6107 (1)	SCR 0914−4134 (1)	SCR 1048−7739 (1)	SCR 1110−3608 (1)	SCR 1125−3834 (1)
SCR 1138−7721 (1)	SCR 1147−5504 (1)	SCR 1157−0149 (1)	SCR 1204−4037 (1)	SCR 1206−3500 (1)	SCR 1206−5019 (1)
SCR 1214−2345 (1)	SCR 1214−4603 (1)	SCR 1217−7810 (1)	SCR 1224−5339 (1)	SCR 1230−3411 (1)	SCR 1233−4826 (1)
SCR 1240−8116 (1)	SCR 1245−5506 (1)	SCR 1247−0525 (1)	SCR 1317−4643 (1)	SCR 1347−7610 (1)	WT 0244 (1)
WT 0392 (1)	WT 1962 (1)				
Unresolved at CTIO (2010.5885−2010.5890)					
CD−587828	CD−616505	GIC129 (1), (4)	GJ 1	GJ 7 (1)	GJ 17.1 (1)
GJ 46 (1)	GJ 54.1 (1)	GJ 57	GJ 84.1 (1)	GJ 91	GJ 114.1
GJ 590 (1)	GJ 592 (1)	GJ 618 (4)	GJ 620	GJ 643 (1), (4)	GJ 660.1 (4)
GJ 674	GJ 680 (4)	GJ 682 (6)	GJ 693	GJ 723 (1)	GJ 739
GJ 741 (1)	GJ 747.1 (1)	GJ 747.4 (1)	GJ 754 (1)	GJ 781.1 (1), (4)	GJ 784 (1)
GJ 788.1 (1)	GJ 803 (4)	GJ 832	GJ 841 (4)	GJ 842	GJ 855 (1)
GJ 871.1 (1), (4)	GJ 874 (1)	GJ 887	GJ 891 (1)	GJ 1016 (1)	GJ 1028 (1)
GJ 1032 (1)	GJ 1212 (1)	GJ 1215 (1)	GJ 1252 (1)	GJ 2138 (1), (3)	GJ 2151 (1)
GJ 2154 (4)	HD 17051	HDS 2941A (1)	HDS 2941B (1)	HIP 88118 (1)	HIP 106803 (1)
HIP 113850 (1)	HJ 3126A (1)	HJ 3126B (1)	HJ 4935C (1)	LDS 18A (1)	LDS 18B (1)
LDS 2375B (1)	LDS 2951A (1)	LDS 2951B (1)	LDS 4929A (1)	LDS 4929B (1)	LDS 6418 (1), (4)
LDS 65A (1)	LDS 65B (1)	LDS 782 (1), (4)	LHS 142 (1)	LHS 406 (1)	LHS 423 (1)
LHS 440 (1)	LHS 499 (1)	LHS 547 (1)	LHS 1339 (1)	LHS 3169 (1)	LHS 3218 (1)
LHS 3315 (1)	LHS 3377 (1)	LHS 3413 (1)	LHS 3492 (1)	LHS 4016 (1)	LHS 5004 (1)
LHS 5303 (1)	LHS 5341 (1)	LP 804-027 (1)	LP 876-034 (1)	LP 984-092 (1), (4)	LTT 464 (1)
LTT 6288 (1)	LTT 6840 (1)	LTT 7138 (1)	LTT 8456 (1)	LTT 8526 (1)	LTT 9455 (1)
MLO 4A	MLO 4B	NLTT 8065 (1)	SCR 0031−3606 (1)	SCR 0128−1458 (1)	SCR 1627−1925 (1)
SCR 1654−0055 (1)	SCR 1816−5844 (1), (4)	SCR 2033−2556 (1)	SCR 2036−3607 (1)	SCR 2049−4012 (1)	SCR 2053−6223 (1)
SCR 2055−6001 (1)	SCR 2116−5825 (1)	WT 1962 (1)			

Note. (1) Observed with wider FWHM filter due to faintness of target. Resolution limit for this observation is estimated at $\rho = 0\farcs05$. (2) Resolved companion has too large a Δm for detection here. (3) Resolved companion. See Section 5 and Appendix. (4) Only brighter component of the resolved pair observed. Fainter component too wide for differential measure here. (5) Detected companion. See Section 5 and Appendix. (6) Companion has only been detected in the infrared. The magnitude difference may be too large for detection in the visible.

The USNO speckle interferometry program has been supported by NASA and the SIM preparatory science program through NRA 98-OSS-007. This research has made use of the SIMBAD database, operated at CDS, Strasbourg, France and NASA's Astrophysics Data System. Thanks are also provided to the U.S. Naval Observatory for their continued support of the Double Star Program. The telescope operators and observing support personnel of KPNO and CTIO continue to provide exceptional support for visiting astronomers. Thanks to Claudio Aguilero, Alberto Alvarez, Skip Andree, Bill Binkert, Gale Brehmer, Ed Eastburn, Angel Guerra, Hal Halbedal, Humberto Orrero, David Rojas, Hernan Tirado, Patricio Ugarte, Ricard Venegas, George Will, and the rest of the KPNO and CTIO staff. Members of the RECONS team (J.P.S. and T.J.H.) have been supported by NSF grants AST 05-07711, 09-08402, and 14-12026. We would also like to thank Andrei Tokovinin for helpful comments.

Appendix A
Additional Measured Pairs

Table 7 presents other, non-M dwarf pairs observed during the runs presented in Table 1. The first two columns identify the system by providing the WDS designation (based on epoch-2000 coordinates) and discovery designation. Columns three through five give the epoch of observation (expressed as a fractional Julian year), the position angle (in degrees), and the separation (in seconds of arc). The sixth column indicates the number of observations contained in the mean position. The last column is reserved for notes for these systems.

Table 7
Speckle Interferometric Measurements of Other Pairs

WDS Designation	Discoverer Designation			JY	θ	ρ	n	Note
$\alpha\delta$ (2000)				2000.+	(∘)	(″)		
(1)	(2)			(3)	(4)	(5)	(6)	(7)
00022+2705	BU	733		07.5992	253.6	0.853	1	
00063+5826	STF	3062		05.8625	338.8	1.520	1	
00063+5826				07.5885	340.8	1.520	1	
00308+4732	BU	394		07.6021	273.9	0.538	1	
00321−0511	A	111		07.6019	131.3	0.144	1	
00352−0336	HO	212		05.8615	276.0	0.282	1	
00352−0336				07.6019	332.1	0.107	1	
01376−0924	KUI	7		05.8656	140.6	0.179	1	
03127+7133	STT	50		07.6022	150.4	1.058	1	
03400+6352	HU	1062	BC	05.8629	39.9	0.207	1	
03562+5939	HDS	497	AD	07.6075	23.6	0.192	1	
04070−1000	HDS	521		05.8665	342.4	0.231	1	
04070−1000				06.1908	341.2	0.225	1	
04070−1000				10.0652	313.0	0.200	1	
04163+0710	WSI	97		06.1909	125.8	0.138	1	
04199+1631	STT	79		05.8633	333.4	0.406	1	
04199+1631				06.1909	337.4	0.395	1	
04227+1503	STT	82		05.8687	337.0	1.285	1	
04256+1556	FIN	342	Aa,Ab	05.8633	83.8	0.100	1	
04258+1800	COU	2682		05.8633	315.6	0.269	1	
04259+1852	BU	1185		05.8633	22.6	0.272	1	
04259+1852				06.1909	22.3	0.246	1	
04290+1610	HU	1080		05.8688	76.2	0.273	1	
04340+1510	CHR	17		05.8658	275.5	0.181	1	
04375+1509	CHR	153		05.8658	115.4:	0.401:	1	
04506+1505	CHR	20		05.8688	297.9	0.123	1	
04512+1104	BU	883		05.8688	117.9	0.123	1	
04512+1104				06.1909	125.4	0.130	1	
07128+2713	STF	1037		05.8636	310.3	1.084	1	
07277+2127	MCA	30	Aa,Ab	05.8636	347.7	0.105:	1	
07480+6018	HU	1247		05.8636	258.8	0.229	1	
07518−1354	BU	101		06.1910	81.7	0.259	1	
08044+1217	BU	581		05.8618	135.2	0.365	1	
08044+1217				06.1910	137.3	0.358	1	
09123+1500	FIN	347	Aa,Ab	05.8636	135.4	0.165	1	
09123+1500			Aa,Ab	06.1910	122.4	0.136	1	
09179+2834	STF	3121		05.8636	204.8	0.758	1	
09252−1258	WSI	73		10.0660	276.7	0.179	1	
11190+1416	STF	1527		06.1941	131.6	0.298	1	
11272−1539	HU	462		06.1941	157.8	0.417	1	
11272−1539				10.0659	133.9	0.406	1	
11317+1422	WSI	101	Aa,Ab	08.4500	14.6:	0.218:	1	
12036−3901	SEE	143		06.1941	49.5	0.664	1	
12036−3901				10.0659	39.0	0.590	1	

Table 7
(Continued)

WDS Designation	Discoverer Designation			JY	θ	ρ	n	Note
$\alpha\delta$ (2000)				2000.+	(°)	(″)		
(1)	(2)			(3)	(4)	(5)	(6)	(7)
12485−1543	WSI	74	Aa,Ab	06.1915	44.6	0.050	1	
12485−1543			Aa,Ab	10.0715	316.0	0.135	1	
13038−2035	BU	341		10.0715	131.7	0.591	1	
13149−1122	RST	3829	Aa,Ab	06.1942	140.3	0.610	1	
13169−3436	I	1567		06.1942	240.0	0.094	1	
13258+4430	A	1609		08.4611	30.9	0.454	1	
13513−2423	WSI	77		06.1890	171.3	0.333	1	(A)
13513−2423				10.0715	350.2	0.209	1	
14020−2108	WSI	79		06.1896	156.8	0.320	1	
14310−0548	RST	4529		06.1917	333.3	0.285	1	
14310−0548				10.5892	0.1	0.280	2	
14492+1013	A	2983		06.1917	346.1	0.122	1	
14589+0636	WSI	81		06.1943	195.5	0.075	1	(A)
14589+0636				08.4554	73.2	0.128	1	
15206+1523	HU	1160		08.4558	87.5	0.253	1	
15232+3017	STF	1937		07.6013	138.4	0.514	1	
15232+3017				08.4611	150.2	0.535	1	
15282−0921	BAG	25	Aa,Ab	06.1918	340.3	0.121	1	
15360+3948	STT	298		07.6013	173.7	0.981	1	
15360+3948				08.4611	176.6	1.020	1	
15453−5841	FIN	234		10.5854	unresolved		1	
16003−2237	LAB	3		10.5853	13.3	0.088	1	
16059+1041	HDS	2273	Aa,Ab	07.6012	199.7	0.466	1	
16348+2145	WSI	105		08.4504	135.9	0.091	1	(A)
17198−3606	WSI	61	Ba,Bb	10.5856	unresolved		1	
17304−0104	STF	2173		06.2000	167.8	0.392	1	
17304−0104				07.6014	159.6	0.550	1	
17304−0104				08.4559	158.0	0.637	1	
17304−0104				10.5908	153.8	0.787	1	
17561+2130	STT	339		08.4586	169.9	4.072	1	
17572+2400	MCA	50		07.6014	157.3	0.089	1	
18126−7340	TOK	58	Aa,Ab	10.5854	unresolved		2	
18455+0530	FIN	332	Aa,Ab	10.5909	311.8	0.160	1	
18455+0530	FIN	332	Ba,Bb	10.5909	unresolved		1	
18455+0530	STF	2375	Aa,B	10.5909	120.6	2.563	1	
18466+3821	HU	1191		07.5878	270.5	0.231	1	
19126+1651	WSI	107	Ca,Cb	08.4561	252.5	0.090	1	(A), (B)
19196+3720	CIA	2		07.6016	350.0	0.088	1	
19196+3720				08.4509	25.0	0.090	1	
19247+0833	WSI	108		08.4615	27.0	0.071	1	(A), (C)
19282−1209	SCJ	22		10.5909	280.3	0.974	1	
19311+5835	MCA	56		07.6016	66.8	0.116	1	
19316+1747	STF	2536		08.4587	115.9	1.779	1	
19391+7625	MLR	224		07.6016	288.0	0.190	1	
20086+8507	WSI	109		07.6041	200.4	0.081	1	
20086+8507				08.4508	174.6:	0.077:	1	
20096+1648	STF	2634		08.4589	14.3	4.126	1	
20311+3333	COU	1962		07.6018	266.0	0.144	1	
20311+3333				08.4563	273.4	0.166	1	
20312+0513	AG	257		08.4535	73.3	1.698	1	
20374+7536	HEI	7		07.5990	231.0	0.675	1	
21145+1000	STT	535		07.6017	18.5	0.301	1	
21214+1020	A	617		07.6017	87.2	0.167	1	
21214+1020				08.4481	80.9	0.137	1	
21543+1943	COU	432	BC	08.4615	17.9	0.188	1	
22266−1645	SHJ	345		10.5861	43.2	1.274	1	
22282+2332	STF	2910		08.4590	332.7	5.482	1	
22388+4419	HO	295		05.8654	153.1	0.296	1	
22388+4419				07.5991	153.2	0.233	1	
22474+1749	WSI	93		08.4615	108.5	0.296	1	(A)
22481−2422	WSI	138		10.5887	144.2	0.524	1	(A), (D)

Table 7
(Continued)

WDS Designation	Discoverer		JY	θ	ρ	n	Note
$\alpha\delta$ (2000)	Designation		2000.+	(∘)	($''$)		
(1)	(2)		(3)	(4)	(5)	(6)	(7)
22564+1727	STF	2957	08.4591	225.1:	4.559:	1	
22586+0921	STT	536	05.8614	164.7	0.199	1	
23189+0524	BU	80	05.8614	208.6	0.362	1	
23189+0524			07.5883	220.9	0.453	1	
23444−7029	WSI	94	10.5864	unresolved		1	

Note. (A) First observation of this pair. (B) We crudely estimate the Δm in V as 3.0. (C) We crudely estimate the Δm in V as 0.5. (D) See Appendix B.

Appendix B
The Problem With WSI 138

This pair was originally associated with LP 876-10. LP 876-10 was examined multiple times (Mamajek et al. 2013), none of which showed any hint of elongation. Tokovinin et al. (2015) also did not detect it. Mamajek et al. effectively ruled this out an optical coincidence between the high proper motion LP 876-10 and a background star. The tentative conclusion is that a different pair was observed and that the 2010 measure (see Table B1) was not of LP 876-10, but instead of some other unidentified pair which may or may not be a physical pair. While no nearby known pairs in the WDS matches the approximate morphology of the pair, in this magnitude range an unknown double star would not be a surprise. As we are unsure what star was examined the WDS does not provide a precise position, the magnitudes of the components are degraded, and it has been disassociated with Fomalhaut.

ORCID iDs

William I. Hartkopf https://orcid.org/0000-0001-6111-4560
John P. Subasavage https://orcid.org/0000-0001-5912-6191

References

Bagnuolo, W. G., Jr., Mason, B. D., Barry, D. J., Hartkopf, W. I., & McAlister, H. A. 1992, AJ, 103, 1399
Balega, I. I., Balega, Yu. Yu., & Malogolovets, E. V. 2010, AstBu, 65, 250
Bartlett, J. L., Lurie, J. C., Riedel, A., et al. 2017, AJ, 154, 151
Benedict, G. F., Henry, T. J., Franz, O. G., et al. 2016, AJ, 152, 141
Delfosse, X., Bonfils, X., Forveille, T., et al. 2013, A&A, 553, 8
Docobo, J. A., Balega, Y. Y., Ling, J. F., Tamazian, V., & Vasyuk, V. A. 2000, AJ, 119, 2422
Docobo, J. A., Tamazian, V. S., Balega, Y. Y., et al. 2008, A&A, 478, 187
ESA 1997, The Hipparcos and Tycho Catalogues (ESA SP-1200) (Noordwijk: ESA)
Forveille, T., Beuzit, J.-L., Delfosse, X., et al. 1999, A&A, 351, 619
Harrington, R. S., & Dahn, C. C. 1988, AJ, 96, 718
Hartkopf, W. I., & Mason, B. D. 2014, IAU DS Circular #184, 1
Hartkopf, W. I., & Mason, B. D. 2015, Catalog of Rectilinear Elements (Washington, D.C.: U.S. Naval Observatory)
Hartkopf, W. I., Mason, B. D., & McAlister, H. A. 1996, AJ, 111, 370
Hartkopf, W. I., Mason, B. D., & Worley, C. E. 2001a, AJ, 122, 3472
Hartkopf, W. I., McAlister, H. A., & Franz, O. G. 1989, AJ, 98, 1014
Hartkopf, W. I., McAlister, H. A., & Mason, B. D. 2001b, AJ, 122, 3480
Hartkopf, W. I., Tokovinin, A., & Mason, B. D. 2012, AJ, 143, 42
Heintz, W. D. 1986, A&AS, 65, 411
Heintz, W. D. 1990, A&AS, 82, 65
Henry, T. J., Franz, O. G., Wasserman, L. H., et al. 1999, ApJ, 512, 864
Henry, T. J., Jao, W.-C., Subasavage., J. P., et al. 2006, AJ, 132, 2360
Horch, E. P., Bahi, L. A. P., Gaulin, J. R., et al. 2012, AJ, 143, 10
Horch, E. P., Falta, D., Anderson, L. M., et al. 2010, AJ, 139, 205
Horch, E. P., Gomez, S. C., Sherry, W. H., et al. 2011, AJ, 141, 45
Jancart, S., Jorrisen, A., Babusiaux, C., & Pourbaix, D. 2005, A&A, 442, 365
Janson, M., Bergfors, C., Brandner, W., et al. 2014a, ApJS, 214, 17
Janson, M., Bergfors, C., Brandner, W., et al. 2014b, ApJ, 789, 102
Janson, M., Hormuth, F., Bergfors, C., et al. 2012, ApJ, 754, 44
Jao, W.-C., Henry, T. J., Subasavage, J. P., et al. 2005, AJ, 129, 1954
Jodar, E., Perez-Garrido, A., Diaz-Sanchez, A., et al. 2013, MNRAS, 429, 859
Kellogg, K., Prato, L., Torres, G., et al. 2017, ApJ, 844, 168
Kervalla, P., Merand, A., Ledoux, C., Demory, B.-O., & Le Bouquin, J.-B. 2016, A&A, 593, 127
Köhler, R., Ratzka, T., & Leinert, Ch. 2012, A&A, 541, 29
Mamajek, E. E., Bartlett, J. L., Seifahrt, A., et al. 2013, AJ, 146, 154
Mason, B. D., & Hartkopf, W. I. 2012, IAU DS Circular #178, 1
Mason, B. D., Hartkopf, W. I., Gies, D. R., Henry, T. J., & Helsel, J. W. 2009, AJ, 137, 3358
Mason, B. D., Hartkopf, W. I., Raghavan, D., et al. 2011, AJ, 142, 176
Mason, B. D., Wycoff, G. L., Hartkopf, W. I., Douglass, G. G., & Worley, C. E. 2001, AJ, 122, 3466, See current version at http://ad.usno.navy.mil/wds/
McAlister, H. A., Hartkopf, W. I., Hutter, D. J., & Franz, O. G. 1987, AJ, 93, 688
Miles, K. N., & Mason, B. D. 2016, IAU DS Circular #190, 1
Montagnier, G., Ségransan, D., Beuzit, J. Ł., et al. 2006, A&AL, 460, 19
Prieur, J.-L., Scardia, M., Pansecchi, L., et al. 2014, AN, 335, 817
Riedel, A. R., Finch, C. T., Henry, T. J., et al. 2014, AJ, 147, 85
Roeser, S., Demleitner, M., & Schilbach, E. 2010, AJ, 139, 2440
Schulz, A. B., Hart, H. M., Hershey, J. L., et al. 1998, PASP, 110, 31
Ségransan, D., Delfosse, X., Forveille, T., et al. 2000, A&A, 364, 665
Söderhjelm, S. 1999, A&A, 341, 121
Tamazian, V. S., Docobo, J. A., Melikian, N. D., Balega, Y. Y., & Karaperian, A. A. 2005, AJ, 130, 2847
Tanner, A. M., Gelino, C. R., & Law, N. M. 2010, PASP, 122, 1195
Tokovinin, A., Mason, B. D., & Hartkopf, W. I. 2010, AJ, 139, 743
Tokovinin, A., Mason, B. D., & Hartkopf, W. I. 2014, AJ, 147, 123
Tokovinin, A., Mason, B. D., Hartkopf, W. I., Mendez, R. A., & Horch, E. P. 2015, AJ, 150, 50
Tokovinin, A., Mason, B. D., Hartkopf, W. I., Mendez, R. A., & Horch, E. P. 2016, AJ, 151, 153
Tokovinin, A., Mason, B. D., Hartkopf, W. I., Mendez, R. A., & Horch, E. P. 2018, AJ, submitted
van Altena, W. F., Lee, J. T., & Hoffleit, E. D. 1995, The General Catalogue of Trigonometric (stellar) Parallaxes (New Haven, CT: Yale Univ. Observatory)
van Leeuwen, F. 2007, A&A, 474, 653
Ward-Duong, K., Patience, J., De Rosa, R. J., et al. 2015, MNRAS, 449, 2618
Winters, J. G., Henry, T., Lurie, J., et al. 2015, AJ, 149, 5
Winters, J. G., Henry, T. J., Jao, W.-C., et al. 2011, AJ, 141, 21
Winters, J. G., Sevrinsky, R. A., Jao, W.-C., et al. 2017, AJ, 153, 14
Zacharias, N., Finch, C., & Frouard, J. 2017, AJ, 153, 166
Zacharias, N., Finch, C. T., Girard, T. M., et al. 2013, AJ, 145, 44
Zirm, H. 2003, IAU DS Circular #151, 1